Patient-derived Sialyl-Tn-positive Invasive Bladder Cancer Xenografts in Nude Mice: An Exploratory Model Study

CARINA BERNARDO[1,9], CÉU COSTA[1,2], TERESINA AMARO[3], MARGARIDA GONÇALVES[1,4], PAULA LOPES[5], RUI FREITAS[6], FÁTIMA GÄRTNER[7,8], FRANCISCO AMADO[9], JOSÉ ALEXANDRE FERREIRA[1,4] and LÚCIO SANTOS[1,2,10]

[1]*Experimental Pathology and Therapeutics Group, Research Center, Portuguese Institute of Oncology Francisco Gentil, Porto, Portugal;*
[2]*Health Faculty, Fernando Pessoa University, Porto, Portugal;*
[3]*Department of Pathology, Hospital Pedro Hispano, Matosinhos, Portugal;*
[4]*Mass Spectrometry Center, QOPNA, Department of Chemistry, University of Aveiro, Aveiro, Portugal;*
Department of [5]*Pathology and* [6]*Urology, Portuguese Institute of Oncology Francisco Gentil, Porto, Portugal;*
[7]*Institute of Pathology and Molecular Immunology of the University of Porto (IPATIMUP), Porto, Portugal;*
[8]*Institute of Biomedical Science Abel Salazar, University of Porto (ICBAS-UP), Porto, Portugal;*
[9]*School of Health Sciences, University of Aveiro (ESSUA), Aveiro, Portugal;*
[10]*Department of Surgical Oncology, Portuguese Institute of Oncology Francisco Gentil, Porto, Portugal*

Abstract. *Background: More than 70% of muscle invasive bladder cancers (MIBC) express the cell-surface antigen sialyl-Tn (sTn) that promotes motility and invasive potential of tumor cells. Effective drug testing models to optimize therapy against these tumors are warranted. Materials and Methods: Fragments of sTn-positive MIBC were subcutaneously engrafted into nude mice and expanded until the third passage. Histology and immunoexpression of tumor markers (p53, p63, Ki-67, CK20, sTn) were studied in order to evaluate tumor phenotype maintenance. Results: Tumor take rate was low in the first passage (1/9) but increased and became consistent, therefore suitable for drug testing, in the third passage (13/13). Histology and immunoexpression patterns were similar between primary tumors and xenografts. However, p53 and ki-67 levels increased with passages suggesting a selection of more proliferative clones. STn expression, even though decreased, was preserved in xenografts. Conclusion: We describe the first patient-derived sTn-positive xenograft model to be used for drug testing and identification of prognostic biomarkers.*

Bladder cancer is the fourth most common genitourinary cancer in men and the seventh in women, with an estimated 386,365 new cases and 150,165 deaths yearly (1).

Although only one-third of the newly-diagnosed bladder carcinomas are advanced at presentation (clinical stage cT2-T4a), 15-30% of high-grade superficial tumors progress to muscle-invasive cancers (MIBC), usually within 5 years (2). The standard treatment for patients with MIBC is radical cystectomy with removal of regional lymph nodes (3). However, up to 50% of patients will relapse with progression to metastatic disease associated with poor survival (4). In order to improve this poor outcome, neoadjuvant chemotherapy with therapeutic regimens containing cisplatin, such as MVAC (methotrexate, vinblastine, doxorubicin and cisplatin) or GC (gemcitabine and cisplatin) are recommended (3, 5). Previous studies have shown that neoadjuvant platinum-based chemotherapeutics were associated to an absolute risk reduction of 8% in 5-years follow-up (6). However, significant variations in the natural history and response to treatment are seen between MIBC tumors with identical histological features, reflecting a heterogeneity of the constituent tumor cells (7). At the moment, there are no biomarkers available to predict MIBC response to chemotherapy or assist to the design of optimal treatment schemes, which would translate to better outcomes, reduced toxicity and improved overall survival.

Abbreviations: H&E: Hematoxylin and eosin; MIBC: muscle invasive bladder cancer; sTn: sialyl-Tn; FFPE, formalin-fixed, paraffin-embedded.

Correspondence to: Lúcio Lara Santos, Experimental Pathology and Therapeutics Group, Portuguese Institute of Oncology Francisco Gentil, Rua Dr. António Bernardino de Almeida 4200-072, Porto, Portugal. Tel: +351 225084000, Fax: +351 225084001, e-mail: llarasantos@gmail.com

Key Words: Human xenografts, urothelial cancer, drug testing, animal models, sialyl-Tn, glycosylation.

Reflecting the molecular heterogeneity of invasive tumors, we recently reported that approximately 70% of MIBCs express the sialyl-Tn (sTn) carbohydrate antigen, resulting from a premature stop in proteins glycosylation. The sTn antigen was observed in highly proliferative tumors and found to promote cell motility and invasive capability (8). The increased expression of ST6GalNac-I leads to STn biosynthesis (9) in several epithelial cancers (*e.g.* gastric, pancreatic, colorectal, ovarian and breast cancers) and is usually associated with poor prognosis (10, 11) Additionally, the sTn antigen contributes to avoidance of metastatic cell elimination in the blood stream by preventing immune recognition (12), while modulating the malignant phenotype (13) and enhancing the metastatic ability of cancer cells (14). Therefore, efficient therapies against sTn-positive bladder tumors are warranted and the response of these particular tumors phenotypes/clones to available chemotherapy agents remains unknown.

The development of non-human models expressing the sTn antigen has been a particularly challenging enterprise. Despite the pan-carcinoma nature of this antigen (10) several well-established cancer cell lines of different organs either do not express, or lose their ability to present this type of glycosylation (8, 15), denoting a dependence of the tumor microenvironment (8). In an attempt to overcome this limitation bio-engineered cell lines expressing the sTn antigen have been successfully xenografted into mice and were shown responsible for enhancing the metastatic capability of cancer cells (13, 15). Recently, the colon cancer cell line LSC that naturally-expresses the sTn antigen was also xenografted into nude mice and shown to be inhibited by the anti-sTn monoclonal antibody 3P9 (16). However, to our knowledge, the direct xenotransplantation of a sTn-positive bladder tumor into nude mice had not, to this moment, been attempted.

Xenograft models have been used as a standard model predicting for efficacy and toxicity of cancer chemotherapeutic agents before entering the clinic due to its ease, low cost, and faster establishment, when compared to the genetic-engineered models (17). In opposition to the xenografts established from cultured cancer cells, where primary cells adapt and suffer a process of natural selection through several passages in culture, direct xenotransplantation of human tumors' fragments preserves the original cell heterogeneity, tumor phenotype and the malignant potential of human tumors (18, 19). Patient-derived xenografts mimic the heterogeneity of human cancers and have demonstrated superior correlation of chemosensitivity and specificity data for individualized therapy (17) with prediction rates of 90% and 97% for chemosensitivity and chemoresistance, respectively (20). Previous studies have used cancer xenograft models as a platform for molecular and histopathology studies and therapeutic development with good results in terms of success rates, preservation of the original characteristics of the primary tumor and predictive value of the model (21-24). Preserving the primary tumor characteristics is essential to ensure for original glycosylation patterns, since they are dependent, on the way the tumor microenvironment regulates the expression of multiple genes within the glycosylation pathways (25-27). Still, no evidence has been presented regarding the preservation of sTn expression patterns of the original tumor in direct xenografts.

As such, the goal of this study was to establish a direct human bladder cancer xenograft model in nude mice conserving the sTn expression of the primary tumor. Such model is regarded of primary importance to identify for drugs and treatment regimens that would better-serve patients with sTn-positive MIBC. It may also be used to test for novel therapies, as well as as a platform to identify markers of tumor response and resistance to drugs.

Materials and Methods

Primary tumor. A fresh tumor specimen was collected at the time of therapeutic radical cystectomy performed to a 69-year-old man with muscle-invasive urothelial carcinoma (MIBC) at IPO Porto that was neither submitted to pre-operative radiotherapy nor neoadjuvant chemotherapy. After surgical excision, tumor tissue was immediately transported to the laboratory in RPMI medium with 1% penicillin/streptomycin. Part of the tumor was cut into pieces of 1-2 mm^3 and engrafted in mice while the rest was fixed in formalin and processed for histological and immunohistochemical analysis.

This study was approved by the ethical committee of the IPO Porto and informed consent was obtained from the patient.

Animals. The experiments were carried out in accordance with the National and European Convention for the Protection of Animals used for experimental and other scientific purposes and related European Directive (2010/63/EU). Nine male nude mice (strain: N:NIH(s) II-nu/nu), aged 6-7 weeks, obtained from the Animal Experimental Unit at IPATIMUP, Porto, Portugal, were transplanted with human primary tumor. After tumor establishment, 3 and 12 nude mice were used for the second and third passage respectively as illustrated in Figure 1. The animals were maintained under sterile conditions throughout the experiment (temperature 24±2˚C, relative humidity 55±5% and a 12-h photoperiod) in polycarbonate cages. They were fed sterilized autoclave rodent food and water *ad libitum*.

Xenograft establishment. A sample of the patient tumor was cut into 1-2 mm^3 fragments and individual pieces were implanted subcutaneously through small horizontal incisions in the scapular regions of anesthetized nude mice. The tumors were excised when they reached a size of approximately 1.5 cm^3, cut into 1-2 mm^3 fragments and transplanted to another group of mice (P1 and P2) using the same method. Animals were anesthetized using isoflurane according to the manufacturer's instructions at the time of transplantation and tumor removal.

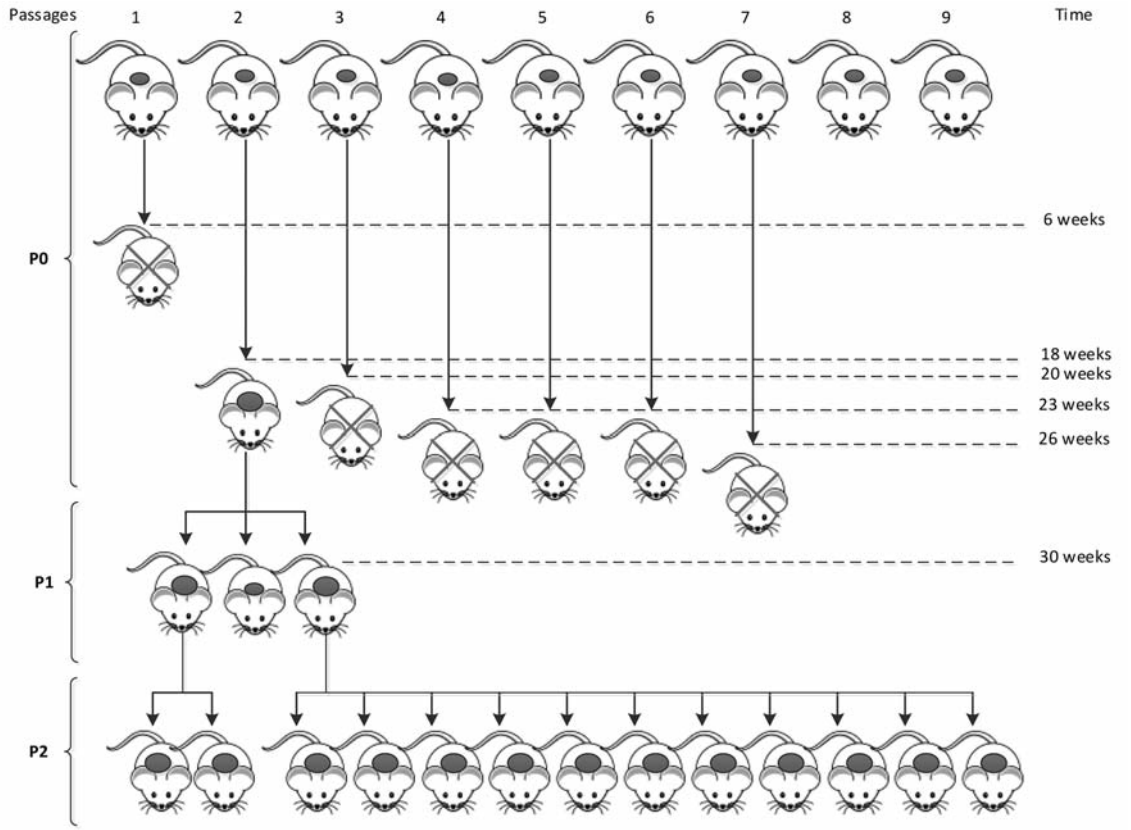

Figure 1. *MIBC tissue was used to establish the xenograft model. After engraftment phase (P0), xenografts were expanded in a cohort of nude mice as described in Materials and Methods. P1 and P2 represent xenografts of second and third generations, respectively. The red crosses represent sacrificed mice without tumor growth, the small red balls represent the tumors implanted, whereas the bigger ones represent tumor growth.*

After transplantation, all mice were observed for development of a palpable mass and tumor growth was assessed using a caliper to determine height (h), width (w) and depth (d) twice a week. Tumor volume was estimated using the formula:

$$Tumor\ volume = \frac{\pi}{6} h * w * d$$

as described elsewhere (28).

Tumor doubling-time (DT) was used for quantification of tumor growth rate. DT was calculated as the time period (t) when the tumor volume was twice (v2) the initial volume (v1) during the exponential phase of tumor growth, using the formula:

$$DT = (t2 - t1) ln2 / \ln\left(\frac{V2}{V1}\right)$$

as defined by Schwartz (29).

Histological analysis. Tissue from the tumors and mice organs was fixed in 10% phosphate buffered formalin, embedded in paraffin, serially-sectioned at 3 μm and stained with hematoxylin-eosin (H&E) for histological examination. Tumors were analyzed in terms of histological type, degree of differentiation, nuclear atypia and extension of invasion whereas mice organs were accessed for tumor metastasis.

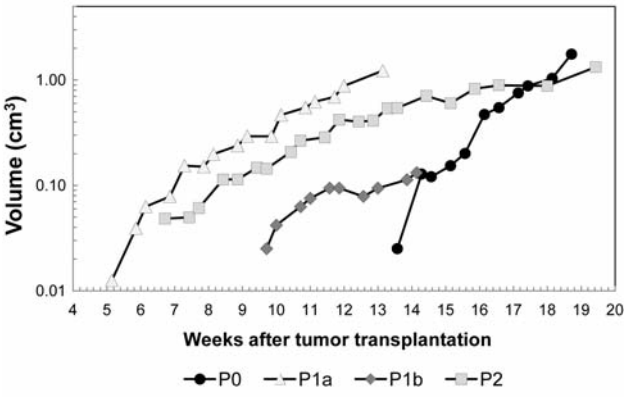

Figure 2. *Tumor growth curve for the first (P0), second (P1) (a and b) and third passage (P2) xenografts. In the first passage the xenograft presented a lag period of 13.5 weeks before progressive tumor growth was observable. The time between transplantation and palpable tumor growth became shorter on subsequent passages, 5 (P1a) and 9 (P1b) weeks in the second passage and around 6 weeks in the third. Xenografts growth rate was regular in the three passages. Different lag periods observed for P1 (P1a and P1b) may be due to different amount of implanted initiating tumor cells. Lag periods and tumor growth rates became more constant in the third passage. Tumor volume was plotted on a logarithmic scale.*

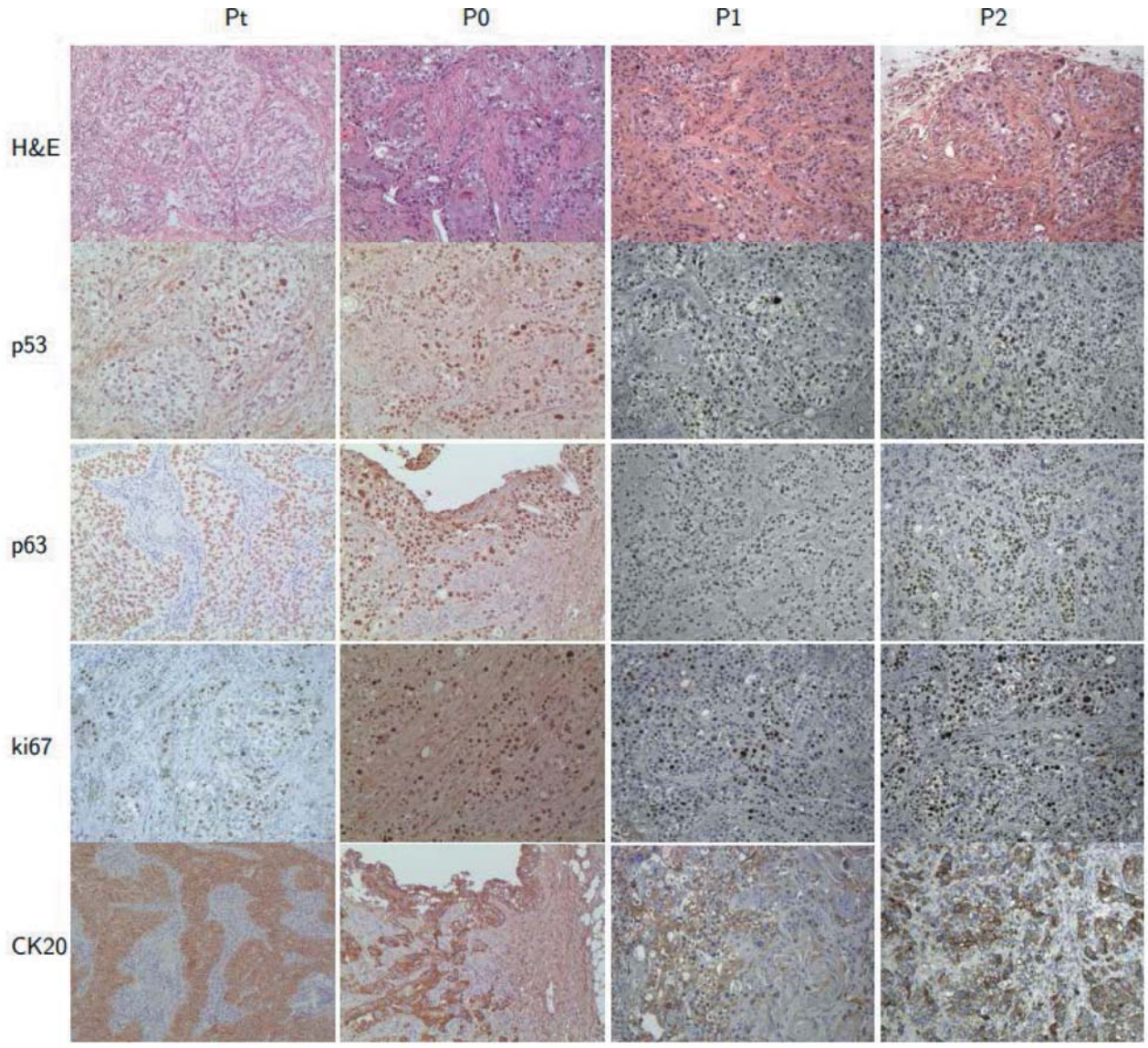

Figure 3. *Histology and tumor molecular markers (p53, p63, ki-67, ck20) immunoexpression of primary tumor (Pt) and first (P0), second (P1), third (P2) generation xenografts (original magnification, ×200). No major differences are seen in the tumor structure and cancer cells markers expression between the original tumor and the xenografts. However in the case of p53 and Ki-67 expression, an increase was observed in xenografts compared to the original tumor, suggesting a more aggressive and proliferative phenotype.*

Immunohistochemical analysis. The primary tumor and the tumors grown in the three passages were tested for molecular marker expression. Formalin-fixed, paraffin-embedded (FFPE) tumor sections (-μm) were tested with primary antibodies against p53 (clone DO -7; Dako, Glostrup, Denmark; 1: 200), p63 (clone 4A4; Dako; 1:300), Ki-67 (clone Mlb-1; Dako; 1:150), CK20 (clone Ks20.8; Novocastra Laboratories Ltd., Newcastle, United Kingdom; 1:150) and sTn (anti-sTn TKH2 monoclonal antibody (30); 1:5 from culture supernatant) using polymer-HRP detection method (Power vision, Duivien, The Netherlands). The sections were initially de-waxed in xylene and rehydrated in a graded series of alcohols. Heat-induced epitope retrieval using citrate buffer was carried out according to antibody manufacturer's instructions. Endogenous peroxidase activity was inhibited by immersing sections in 0.6% H_2O_2 in distilled water for 20 min. Sections were rinsed in PBS-Tween prior to incubation with bovine serum albumin solution (20 min) to inhibit non-specific binding. PBS was subsequently used to wash sections between stages. Sections were then incubated with the primary antibodies against p53, p63, Ki-67, CK20 and sTn. The bound primary antibody was detected by the addition of secondary antibody conjugated with horseradish peroxidase polymer (Power Vision poly-HRP-anti Ms/Rb/R IgG) for 30 min and DAB substrate for 7 min. Then, the slides were counter-stained with hematoxylin and mounted. Positive and negative controls were run simultaneously

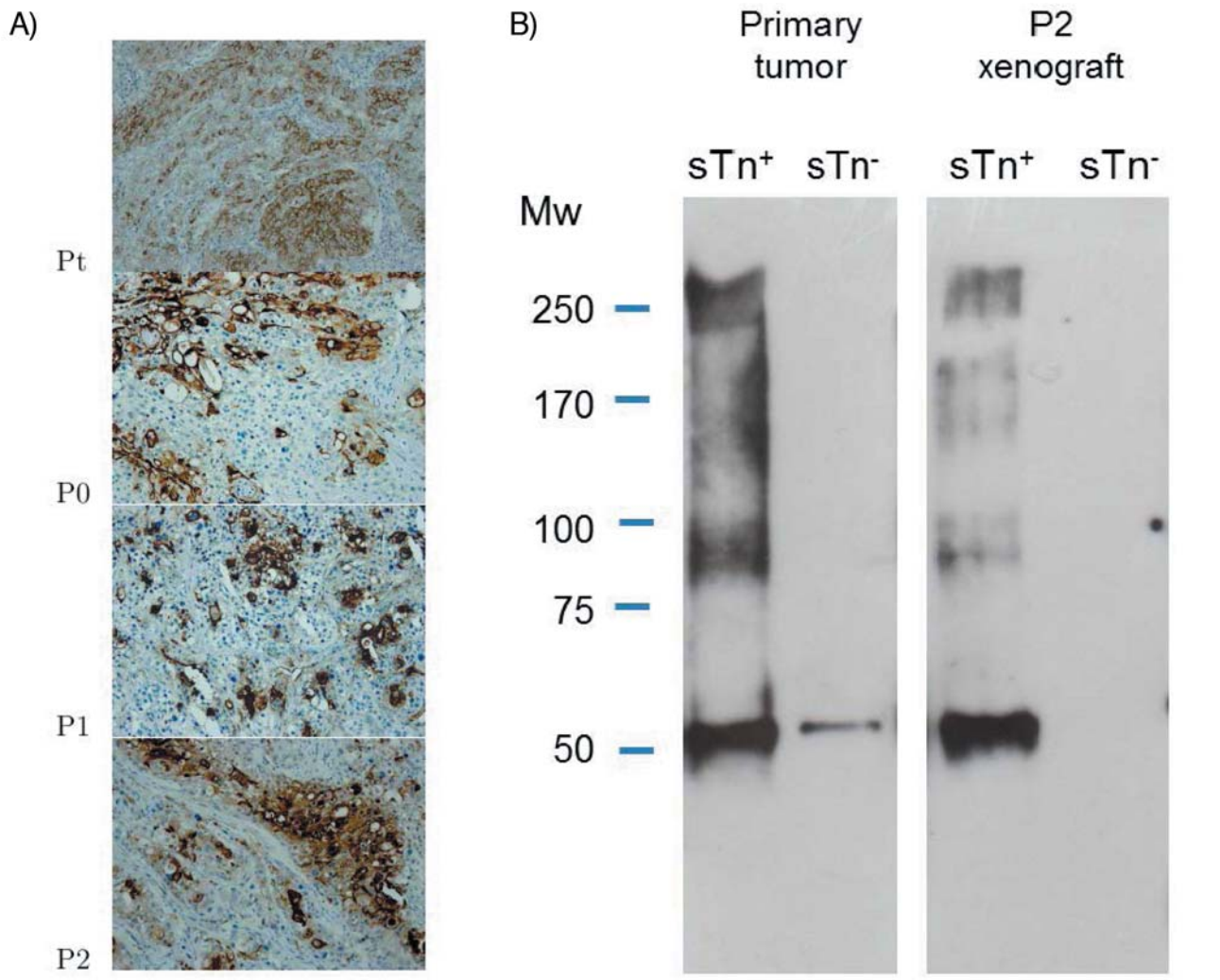

Figure 4. *A, STn immunoexpression in primary tumor and xenografts at first (P0), second (P1) and third generations (P2) (original magnification, ×200). STn expression was maintained, even though decreased, in the xenografts. B, Western blot for the proteins expressing the sTn antigen in primary tumor and P2 xenografts. Similar protein patterns were observed in both cases; differences in staining intensities are thought to results from the lower expression of sTn in xenografts. sTn⁺ refers to the native protein extracts while sTn⁻ refers to protein extracts after de-sialylation with a neuraminidase, which impairs recognition by anti-sTn monoclonal antibody. The absence of immunoreactivity in the sTn⁻ bands confirms the specificity of the recognition pattern.*

with tumor specimens. The expression of sTn was further validated by observing the loss of reactivity with anti-sTn monoclonal antibody TKH2 after treatment of the tumor with a neuraminidase from *Clostridium perfringens* (Sigma-Aldrich), as previously described by Marcos *et al*. (11). This treatment was responsible by removing the sialic acid from sTn that impaired antibody recognition.

The staining patterns were assessed by two independent observers (one of them a pathologist) using standard light microscopy. Positive staining was considered when more than 10% of tumor cells showed reactivity. Stain intensity and percentage of tumor cells stained were recorded to each tumor marker and classified into categories A (<25%), B (25-50%), C (50-75%), D (>75%) according to the number of positive tumor cells stained. The Wilcoxon sign rank test was applied to disclose differences between the levels of expression of tumor markers in the primary tumor and xenografts using Stata 12.1 for Windows (Stata Corp LP, Texas, USA).

Protein extraction and western blotting. Proteins were extracted from FFPE tissues using the Qproteome FFPE tissue kit (Qiagen, Germantown, Maryland, USA). The amount of protein in each extract was estimated with RC protein assay kit (Bio-Rad Laboratories, CA, USA). Thirty micrograms of protein were separated by 4-16% gradient SDS–PAGE under reducing conditions and transferred onto 0.45-μm nitrocellulose membranes (Ge Healthcare Uk Ltd., Buckinghamshire, UK). Membranes were blocked with 1% carbohydrate depleted carbo-free solution (Vector Laboratories, Inc., Burlingame, CA, USA) for 1 h at room

temperature, incubated overnight at 4˚C with anti-sTn TKH2 monoclonal antibody in culture supernatant, washed with TBS-T for 30 min, and finally incubated for 45 h with goat anti-mouse IgG1 heavy chain horseradish peroxidase conjugate (Abcam; 1:35,000 in TBS). After washing, the bound antibodies were revealed by chemiluminescence using the ECL prime Kit (Bio-Rad). Samples previously desialylated, as described by Marcos *et al*. (11), were used as controls.

Results

A direct human bladder cancer xenograft model was established (P0) and expanded (P1) in a cohort of nude mice until the third passage (P2) as schematized in Figure 1.

The primary tumor used to establish the xenografts was obtained after radical cystectomy performed to a 69-year-old man diagnosed with invasive urothelial bladder cancer (pT3aN0M0). Histological analysis presented a high-grade urothelial carcinoma invading the muscularis propria and peri-vesical fat (pT3a). Regional lymph nodes and surgical margins were tumor-free. Preliminary analysis by immunohistochemistry showed an intense and diffuse sTn-expression pattern throughout the tumor (>70% positive) including cells invading the muscle and fat layers. Few cells in the tumor-adjacent mucosa were also positive whereas stromal cells were negative. Staining was observed in the cytoplasm, mainly in the *trans*-Golgi region and was particularly intense in the cell membrane, thus in accordance to our previous observations (8).

In the first passage (P0) one out of 9 mice showed tumor growth, which corresponded to a success take rate of 11%. The percentage of successful engraftment increased in sequential passages (2/3 in P1 and 12/12 in P2). The lag period was 4 months for the first passage, and became shorter in subsequent passages, 5-9 weeks in the second and around 9 weeks in the third (Figure 2). Of note, despite certain variance in the lag period between xenografts in the third passage, the tumor growth curves became more similar and constant among them, suggesting consistency in tumor growth. Tumor doubling-time was approximately 6 days in the first generation and became longer in subsequent passages; around 10 and 14 days in the second and third passage respectively. The mice bearing tumors in the three passages had no macroscopic evidence of invasion of adjacent tissues at the time of tumor excision neither metastasis was found at the time of sacrifice.

The establishment of tumors with high successful take rate and homogeneous growth, suitable for drug testing studies, was achieved at the third generation (P2), 8 months after the xenotransplantation of the primary tumor.

Histological and immunohistochemical analysis of the primary tumor and xenografts. The morphological characteristics of xenografs were analyzed and compared to those of the primary tumor. Histology of the original tumor revealed an invasive urothelial bladder carcinoma with high nuclear-to-cytoplasmic ratio, nuclear atypia and presence of mitotic figures. The resulting xenografts presented identical histological features to those observed in the primary tumor, particularly in terms of cellular type and grade of atypia. The percentage of necrosis was around 10% in both the primary tumor and xenografts and some xenografts presented scamous differentiation that ranged between 10 and 25%.

In addition to the neoplasic cells, the first passage xenograft also presented a cyst covered by a layer of epithelial-like cells, which also enclosed the tumor. This vesicle-like sac was composed by an epithelial lining layer of variable number of cells and dense connective tissue and represents the heterogeneity of the tumor cells implanted. This structure was no longer present in subsequent passages, denoting some degree of clonal selection for malignant cells.

The primary tumor and xenografts were further evaluated by immunohistochemistry in relation to proliferation (Ki-67), aggressiveness (p53) and differentiation (p63 and CK20) markers (Figure 3) and sTn antigen expression (Figure 4), whose overexpression is common in aggressive bladder cancer (31).

Both the primary and the xenografted tumors (P0, P1 and P2) were positive for these markers, reinforcing the homology suggested by histological analysis (Figures 3 and 4). Likewise, the primary tumors and the xenografts shared a strong and diffuse expression of p63 and CK20 (>75% of the tumor area), representing similar degrees of differentiation (Table I and Figure 5). However, significant variations were observed in the levels of p53, Ki-67 and sTn between the primary tumor and xenografts and also between sequential passages (Figure 5). In general, the percentage of p53-positive cells was higher in xenografts when compared to the primary tumor (25-75% and 10-25% respectively). This tendency was particularly pronounced in the third generation xenografts. The levels of Ki-67 immunoexpression were also significantly elevated in P0 in comparison to the primary tumor (50-75% and 25-50% respectively). Some variations in Ki-67 expression were also observed between xenografts in different passages (Figure 5). P0 presented the highest proliferative index, in agreement with the lower tumor doubling-time presented by the first-generation xenografts (Figure 2). The expression of Ki-67 decreased in P1 to levels similar to the initial tumor but increased again in P2. Altogether, these data suggest that the xenograft establishment process may be accompanied by the selection of a more aggressive and proliferative phenotype characterized by a significant overexpression of Ki-67 and p53 (Table I).

The sTn antigen, that was highly expressed in the primary tumor (>75% of the area), was also detected in xenografts (Figure 4A); however its levels decreased with xenotransplantation and along consecutive passages. Since

Table I. *Comparison of immunoexpression for tumor markers p53, p63, Ki-67, CK20 and sTn in primary tumor and third generation xenografts (P2).*

Expression levels	Primary tumor	P2 Xenografts	*p*-Value[a]
p53			
A	1 (100%)	1 (8%)	
B	0	4 (33%)	
C	0	6 (50%)	0.0021
D	0	1 (8%)	
p63			
A	0	0	
B	0	0	
C	0	1 (8%)	0.3173
D	1 (100%)	11 (92%)	
Ki-67			
A	0	0	
B	1 (100%)	6 (50%)	
C	0	6 (50%)	0.0143
D	0	0	
CK20			
A	0	0	
B	0	0	
C	0	1 (%)	0.3173
D	1 (100%)	11 (92%)	
sTn			
A	0	5 (42%)	
B	0	6 (50%)	
C	1 (100%)	1 (8%)	0.0020
D	0	0	

[a]Wilcoxon sign rank. Percentage of expression: A (< 25%), B (25-50%), C (50-75%), D (>75%).

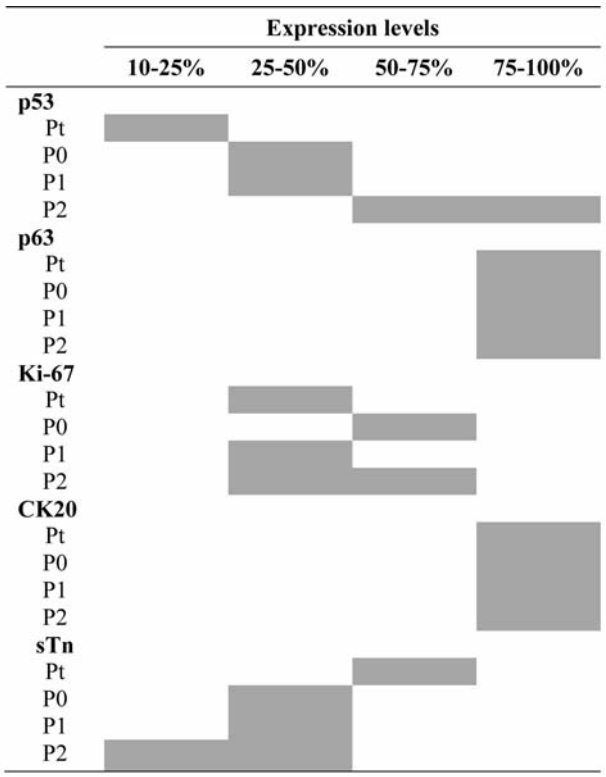

Figure 5. *Immunoexpression of tumor markers p53, p63, Ki-67, CK20 and sTn in the primary tumor (Pt) and first (P0), second (P1) and third (P2) generation xenografts. The expression levels of p63 and CK20 presented by the primary tumor were conserved in the xenografts, indicating similar levels of differentiation. The expression of p53 was increased the xenografts in relation to the primary tumor and increased with sequential passages. Ki-67 increased in P0 but decreased in P1 denoting a process of adaptation of the tumor cells to the host environment. This proliferation indicator then increased in P2, suggesting the selection of high proliferative clones. sTn antigen expression was decreased in the xenografts compared to the primary tumor and decreased with the passages.*

the sTn antigen is a post-translational modification common to several cell-surface glycoproteins, we have also evaluated whether the protein pattern of expression remained conserved in the P2 xenografts by western blot (Figure 4B). Both blots presented a dominant band at approximately 55 kDa and several high-molecular weight bands above 75 kDa that were no longer observable in control experiments with desialylated protein extracts. Therefore, even though decrease in relation to the primary tumor, the expression pattern of sTn remains conserved in the P2 xenografts proteins (Table I).

Discussion

We recently reported that a significant percentage of MIBC expressed the sTn carbohydrate antigen, a post-translational modification of cell-surface proteins responsible by enhancing the motility and invasive capability of bladder cancer cells (8). Therefore, the goal of the present study was to establish a direct human bladder cancer xenograft model in nude mice conserving sTn expression of the primary tumor. Such a model is regarded of primary importance to identify drugs and treatment regimens (32) that would better-serve patients with sTn-positive MIBC.

Herein, we described the transplantation of freshly-collected sTn-positive MIBC fragments directly into nude mice that were then passed to other mice without compromising the histological and molecular nature of the original tumor. Tumor take rate and the consistency in growth rates following implantation, critical aspects of xenograft models, have also been evaluated. In our study, one sample of MIBC was implanted into 9 nude mice with a success take rate of 1/9 (~11%) that increased in subsequent passages. Analogous success rates have been described in previous studies using similar methods for establishing bladder cancer xenografts, independent of

primary tumor stage. Namely, Hay *et al*., reported a success take rate of 7/48 (0.15%) after bilateral transplantation of bladder cancer specimens into 5 immunocompetent mice previously subjected to thymectomy and whole-body radiation (33). Kovnat *et al*., using the same procedure reported a success take rate of 8/33 (0.24%) and 20/53 (0.38%) (34, 35). More recently, Abe *et al*. reported an overall success rate in xenograft establishment of 62.5% (15/24) using severe combined immunodeficient mice and one or two fragments of 4-5 mm^3 per mice (36). In order to increase the tumor take rate, some aspects may be modulated in future xenografts, specifically the number and volume of implanted fragments.

The lag period was 4 months for the first generation xenografts and became shorter on subsequent passages; 5-9 weeks in the second and around 9 weeks in the third. The longer lag period observed in the first passage might be explained by the presence of a low fraction of clonogenic cells in the implanted fragment and the need to adapt and grow in a new environment. The xenografts' growth rates were also different between passages, however, they became similar between xenografts of the same passage in the third generation (P2), suggesting growth consistency. This aspect enables for comparison of tumor growth between groups and assessment of tumor response to chemotherapeutic drugs. These results are in agreement with a previous reports using similar methods (human bladder cancer specimen nude mice and subcutaneous implantation) to obtain xenografts from bladder tumors (36) as well as with other cancer xenograft models (19, 24, 32, 37).

Histological analyses have demonstrated high similarity between primary tumors and xenografts in terms of cellular type and grade of atypia, suggesting that the phenotype of the primary tumor is preserved during tumor establishment and expansion in nude mice. This observation was re-inforced by the detection of similar levels of differentiation markers p16 and CK20. However, variations in the expression of p53 and Ki-67 were observed between the primary tumor and the xenografts and between different passages. A comparison between primary tumor and third generation xenografts has further highlighted an increased expression of p53 and Ki-67, suggesting a tendency to select for the most aggressive and rapidly-growing cells from a heterogeneous primary tumor during the engraftment process. In accordance with these observations, several publications have described that certain cell populations of the primary tumor can be amplified by the xenografting process and may represent the natural tumor evolving process towards a more aggressive phenotype with higher potential to adapt and metastasize (38, 39). Along with the ability to obtain high take rate and stable tumor growth, these events re-inforced the value of third-generation xenografts and subsequent passages as a good model for cancer drug testing.

We also observed that xenografts reproduced the sTn expression pattern observed in the primary tumor, thereby creating the first *in vivo* bladder tumor model expressing this antigen. The development of non-human models expressing the sTn antigen has been a particularly challenging enterprise. Despite the pan-carcinoma nature of this antigen (10), *in vivo* models that mimic clinical setting of tumors expressing this antigen are still missing and the direct xenotransplantation of a sTn-positive human bladder tumor cells into nude mice had not yet been attempted. In our model sTn antigen expression decreased in xenografts in comparison to the primary tumor, a decrease that became more pronounced in the third generation which also showed a more prominent proliferative phenotype. Such observations re-inforce our previous findings that, despite being associated with proliferative phenotypes, cells expressing sTn antigens are commonly found in non-proliferative invasive areas of the tumor. Nevertheless, third generation xenografts conserved significant sTn expression and presented an sTn-expressing glycoprotein profile similar to the primary tumor. Studies are ongoing to determine the nature of these proteins and disclose the environmental factors that promote sTn expression in bladder cancer.

Given their capability to recapitulate the histological and molecular nature of the primary tumor, the sTn-expressing bladder cancer xenografts show potential as a model to determine the adequate treatment schemes for these tumors, test new drugs and identify prognostic biomarkers. Similar xenograft models for other cancers have shown a "remarkable correlation between drug activity in the model and clinical outcome" and have already been transpose into the clinical practice (24). Altogether we believe that this approach may also be useful in the context of MIBC. Additional work involving a larger patient cohort is ongoing to optimize the model and further explore its potential in drug testing. Given the pancarcinoma nature of sTn antigen expression, its association with invasion and metastases, these findings may constitute valuable insights for other tumors.

Acknowledgements

This work study was supported by the Portuguese Foundation for Science and Technology (FCT) PhD grant SFRH/BD/80855/2011 (CB) and Postdoctoral grant SFRH/BPD/66288/2009 (JAF) and by the "Associação Portuguesa de Urologia". FCT is cofinanced by the European Social Fund (ESF) under Human Potential Operation Programme (POPH) from National Strategic Reference Framework (NSRF). The authors also thank professor Celso A. Reis (IPATIMUP, Portugal) for kindly providing the anti-sTn monoclonal antibody TKH2 used in this study.

References

1 Ferlay J, Shin H-R, Bray F, Forman D, Mathers C and Parkin DM: Estimates of worldwide burden of cancer in 2008: GLOBOCAN 2008. Int J Cancer *127(12)*: 2893-2917, 2010.

2 Sylvester RJ, van der Meijden APM, Oosterlinck W, Witjes JA, Bouffioux C, Denis L, Newling DWW and Kurth K: Predicting recurrence and progression in individual patients with stage Ta T1 bladder cancer using EORTC risk tables: a combined analysis of 2596 patients from seven EORTC trials. Eur Urol *49(3)*: 466-477, 2006.

3 Witjes JA, Compérat E, Cowan NC, Santis M De, Gakis G, Lebret T, Ribal MJ and Sherif A: Guidelines on bladder cancer: muscle-invasive and metastatic. Eur Assoc Urol, 2013.

4 Advanced Bladder Cancer (ABC) Meta-analysis Collaboration, C Vale: Neoadjuvant chemotherapy in invasive bladder cancer: a systematic review and meta-analysis. Lancet *361(9373)*: 1927-1934, 2003.

5 Bellmunt J, Albiol S, Kataja V; ESMO Guidelines Working Group: Invasive bladder cancer: ESMO clinical recommendations for diagnosis, treatment and follow-up. Ann Oncol *20(Suppl 4)*: 79-80, 2009.

6 Sherif A, Holmberg L, Rintala E, Mestad O, Nilsson J, Nilsson S and Malmström P-U: Neoadjuvant cisplatinum based combination chemotherapy in patients with invasive bladder cancer: a combined analysis of two Nordic studies. Eur Urol *45(3)*: 297-303, 2004.

7 Spruck CH, Ohneseit PF, Gonzalez-Zulueta M, Esrig D, Miyao N, Tsai YC, Lerner SP, Schmütte C, Yang S and Cote R: Two molecular pathways to transitional cell carcinoma of the bladder. Cancer Res *54(3)*: 784-788,1994.

8 Ferreira JA, Videira P a, Lima L, Pereira S, Silva M, Carrascal M, Severino PF, Fernandes E, Almeida A, Costa C, Vitorino R, Amaro T, Oliveira MJ, Reis CA, Dall'olio F, Amado F and Santos LL: Overexpression of tumour-associated carbohydrate antigen sialyl-Tn in advanced bladder tumours. Mol Oncol *7(3)*: 719-731, 2013.

9 Marcos NT, Pinho S, Grandela C, Cruz A, Samyn-Petit B, Harduin-Lepers A, Almeida R, Silva F, Morais V, Costa J, Kihlberg J, Clausen H and Reis CA: Role of the human ST6GalNAc-I and ST6GalNAc-II in the synthesis of the cancer-associated sialyl-Tn antigen. Cancer Res *64(19)*: 7050-7057, 2004.

10 Julien S, Videira PA and Delannoy P: Sialyl-Tn in Cancer: (How) Did We Miss the Target? Biomolecules *2(4)*: 435-466, 2012.

11 Marcos NT, Bennett EP, Gomes J, Magalhaes A, Gomes C, David L, Dar I, Jeanneau C, DeFrees S, Krustrup D, Vogel LK, Kure EH, Burchell J, Taylor-Papadimitriou J, Clausen H, Mandel U and Reis CA: ST6GalNAc-I controls expression of sialyl-Tn antigen in gastrointestinal tissues. Front Biosci (Elite Ed) *3*: 1443-1455, 2011.

12 Ogata S, Uehara H, Chen A and Itzkowitz SH: Mucin Gene Expression in Colonic Tissues and Cell Lines. Cancer Res *52*: 5971-5978, 1992.

13 Pinho S, Marcos NT, Ferreira B, Carvalho AS, Oliveira MJ, Santos-Silva F, Harduin-Lepers A and Reis CA: Biological significance of cancer-associated sialyl-Tn antigen: modulation of malignant phenotype in gastric carcinoma cells. Cancer Lett *249(2)*: 157-170, 2007.

14 Ozaki H, Matsuzaki H, Ando H, Kaji H, Nakanishi H, Ikehara Y and Narimatsu H: Enhancement of metastatic ability by ectopic expression of ST6GalNAcI on a gastric cancer cell line in a mouse model. Clin Exp Metastasis *29(3)*: 229-238, 2012.

15 Julien S, Krzewinski-Recchi MA, Harduin-Lepers A, Gouyer V, Huet G, Le Bourhis X and Delannoy P: Expression of sialyl-Tn antigen in breast cancer cells transfected with the human CMP-Neu5Ac: GalNAc alpha2,6-sialyltransferase (ST6GalNac I) cDNA. Glycoconj J *18(11-12)*: 883-893, 2003.

16 An Y, Han W, Chen X, Zhao X, Lu D, Feng J and Yang D: A Novel Anti-sTn Monoclonal Antibody 3P9 Inhibits Human Xenografted Colorectal Carcinomas. J Immunother *36(1)*: 20-28, 2012.

17 Pathak AK, Bhutani M, Saintigny P and Mao L: Heterotransplant mouse model cohorts of human malignancies: A novel platform for Systematic Preclinical Efficacy Evaluation of Drugs (SPEED). Am J Transl Res *1(1)*: 16-22, 2009.

18 Johnson JI, Decker S, Zaharevitz D, Rubinstein L V, Venditti JM, Schepartz S, Kalyandrug S, Christian M, Arbuck S, Hollingshead M and Sausville EA: Relationships between drug activity in NCI preclinical *in vitro* and *in vivo* models and early clinical trials. Br J Cancer *84(10)*: 1424-1431, 2001.

19 Rubio-Viqueira B and Hidalgo M: Direct *in vivo* xenograft tumor model for predicting chemotherapeutic drug response in cancer patients. Clin Pharmacol Ther *85(2)*: 217-221, 2009.

20 Fiebig HH, Maier A, and Burger AM: Clonogenic assay with established human tumour xenografts: correlation of *in vitro* to *in vivo* activity as a basis for anticancer drug discovery. Eur J Cancer *40(6)*: 802-820, 2004.

21 Jimeno A, Feldmann G, Suárez-Gauthier A, Rasheed Z, Solomon A, Zou G-M, Rubio-Viqueira B, García-García E, López-Ríos F, Matsui W, Maitra A and Hidalgo M: A direct pancreatic cancer xenograft model as a platform for cancer stem cell therapeutic development. Mol Cancer Ther *8(2)*: 310-314, 2009.

22 Chahinian AP, Mandeli JP, Gluck H, Naim H, Teirstein AS and Holland JF: Effectiveness of cisplatin, paclitaxel, and suramin against human malignant mesothelioma xenografts in athymic nude mice. J Surg Oncol *67(2)*: 104-111, 1998.

23 Russell PJ, Raghavan D, Gregory P, Philips J, Wills EJ, Jelbart M, Wass J, Zbroja RA and Vincent PC: Bladder cancer xenografts: a model of tumor cell heterogeneity. Cancer Res *46(4 Pt 2)*: 2035-2040, 1986.

24 Hidalgo M, Bruckheimer E, Rajeshkumar N V, Garrido-Laguna I, De Oliveira E, Rubio-Viqueira B, Strawn S, Wick MJ, Martell J and Sidransky D: A pilot clinical study of treatment guided by personalized tumorgrafts in patients with advanced cancer. Mol Cancer Ther *10(8)*: 1311-1316, 2011.

25 Serpa J, Mesquita P, Mendes N, Oliveira C, Almeida R, Santos-Silva F, Reis CA, LePendu J and David L: Expression of Lea in gastric cancer cell lines depends on {FUT3} expression regulated by promoter methylation. Cancer Lett *242(2)*: 191-197, 2006.

26 Escrevente C, Machado E, Brito C, Reis CA , Stoeck A, Runz S, Marmé A, Altevogt P and Costa J: Different expression levels of alpha3/4 fucosyltransferases and Lewis determinants in ovarian carcinoma tissues and cell lines. Int J Oncol *29(3)*: 557-566, 2006.

27 Sewell R, Bäckström M, Dalziel M, Gschmeissner S, Karlsson H, Noll T, Gätgens J, Clausen H, Hansson GC, Burchell J and Taylor-Papadimitriou J: The ST6GalNAc-I sialyltransferase localizes throughout the Golgi and is responsible for the synthesis of the tumor-associated sialyl-Tn O-glycan in human breast cancer. J Biol Chem *281(6)*: 3586-3594, 2006.

28 Tomayko MM and Reynolds CP: Determination of subcutaneous tumor size in athymic (nude) mice. Cancer Chemother Pharmacol *24(3)*: 148-154, 1989.
29 Schwartz M: A biomathematical approach to clinical tumor growth. Cancer. Wiley Subscription Services, Inc., A Wiley Company *14(6)*: 1272-1294, 1961.
30 Kjeldsen T, Clausen H, Hirohashi S, Ogawa T, Iijima H and Hakomori S: Preparation and Characterization of Monoclonal Antibodies Directed to the Tumor-associated O-linked Sialosyl-2 6 α-N-Acetylgalactosaminyl (Sialosyl-Tn) Epitope. Cancer Res *48(8)*: 2214-2220, 1988.
31 Compérat E, Camparo P, Haus R, Chartier-Kastler E, Bart S, Delcourt A, Houlgatte A, François R, Capron F and Vieillefond A: Immunohistochemical expression of p63, p53 and MIB-1 in urinary bladder carcinoma. A tissue microarray study of 158 cases. Virchows Arch *448(3)*: 319-324, 2006.
32 Tentler JJ, Tan AC, Weekes CD, Jimeno A, Leong S, Pitts TM, Arcaroli, John J, Messersmith WA and Eckhardt SG: Patient-derived tumour xenografts as models for oncology drug development. Nat Rev Clin Oncol *9(6)*: 338-350, 2012.
33 Hay JH, Busuttil A, Steel CM and Duncan W: The growth and histological characteristics of a series of human bladder cancer xenografts. Radiother Oncol *7(4)*: 331-340, 1986.
34 Kovnat A, Buick RN, Connolly JG, Jewett MA, Keresteci AG and Tannock IF: Comparison of Growth of Human Bladder Cancer in Tissue Culture or as Xenografts with Clinical and Pathological Characteristics. Cancer Res *44(6)*: 2530-2553, 1984.
35 Kovnat A, Armitage M and Tannock I: Xenografts of Human Bladder Cancer in Immune-Deprived Mice. Cancer Res *42(9)*: 3696-3703, 1982.
36 Abe T, Tada M, Shinohara N, Okada F, Itoh T, Hamada J-I, Harabayashi T, Chen Q, Moriuchi T and Nonomura K: Establishment and characterization of human urothelial cancer xenografts in severe combined immunodeficient mice. Int J Urol *13(1)*: 47-57, 2006.
37 Ito D, Fujimoto K, Mori T, Kami K, Koizumi M, Toyoda E, Kawaguchi Y and Doi R: *In vivo* antitumor effect of the mTOR inhibitor CCI-779 and gemcitabine in xenograft models of human pancreatic cancer. Int J Cancer *118(9)*: 2337-2343, 2006.
38 Talmadge JE: Clonal Selection of Metastasis within the Life History of a Tumor. Cancer Res *67(24)*: 11471-11475, 2007.
39 Clappier E, Gerby B, Sigaux F, Delord M, Touzri F, Hernandez L, Ballerini P, Baruchel A, Pflumio F and Soulier J: Clonal selection in xenografted human T cell acute lymphoblastic leukemia recapitulates gain of malignancy at relapse. J Exp Med *208*: 653-661, 2011.

Received November 28, 2013
Revised January 10, 2014
Accepted January 14, 2014